Contents lists available at ScienceDirect

Extreme Mechanics Letters

Characterization of hydrogel structural damping

Bohan Wang [a,1], Adriane G. Moura [a,1], Jiehao Chen [a], Alper Erturk [a], Yuhang Hu [a,b,*]

[a] George W. Woodruff School of Mechanical Engineering, Georgia Institute of Technology, Atlanta, GA 30332, United States of America
[b] School of Chemical and Biomolecular Engineering, Georgia Institute of Technology, Atlanta, GA 30332, United States of America

ARTICLE INFO

ABSTRACT

Gels are composed of crosslinked polymer networks and solvent molecules imbibed into the networks. Gels are both ubiquitous in nature and important engineering materials widely used in many applications. Due to their biocompatibility, stimuli-responsiveness, and compliance, gels gain an edge over traditional materials, such as metals and composites in many modern engineering applications. In the past, the static and kinetic properties of gels have been widely studied. However, the dynamic properties of gels, particularly their structural damping, remain largely unknown even though gels are often under dynamic conditions in various applications. The literature of soft materials is lacking both damping data for hydrogels and a standard testing method to that end. This work reports experimentally identified structural damping data for a set of hydrogel samples via resonant vibration tests for the first bending mode. Beam-shaped samples of rectangular cross-section are clamped vertically at both ends and tested under linear base excitation. An analysis of the frequency response functions based on the Euler–Bernoulli beam theory is conducted to extract Young's modulus and structural damping factor. In the experiments, polyacrylamide gels of three different compositions and polydimethylsiloxane (PDMS) elastomers of two different compositions are prepared and tested. The remarkable result is that the hydrogels have 80% less damping than PDMS, even though hydrogels are an order of magnitude softer than PDMS. The molecular origins of the structural damping of hydrogels and PDMS are discussed. The low damping of gels may open new avenues of research and applications of soft materials in structural dynamics and wave propagation, such as metamaterials and topological insulators, among others.

© 2020 Published by Elsevier Ltd.

1. Introduction

Gels are aggregates of cross-linked polymer networks and solvent molecules (Fig. 1a). They are ubiquitous in nature. Most soft biological components, from cells, tissues to organs, are gel-like materials. They play indispensable roles in basic biological functions. Gels are also important engineering materials. The synthetic polymer networks of the gels support an osmotic pressure difference between internal and external solvent, enabling selective solvent molecules to migrate in or out. Many gels are made stimuli-responsive. They can swell or de-swell in response to the external environment, such as relative humidity [1], temperature [2], pH [3], light [4], glucose [5,6], and electric field [7]. Because of the good biocompatibility and universal stimuli-responsiveness, gels have been used in many engineering fields, such as microfluidics [8], drug delivery [9,10], tissue engineering [11], sensors [12,13], actuators [14–16], wearable electronics [17,18], tissue phantoms [19], among others.

In many cases, both the living organs and synthetic gels are often exposed to dynamic conditions, such as vibration [20], impact [21,22], explosion [23,24], and ultrasonic diagnostics [25, 26]. Recently, there has been an increasing interest in realizing elastic/acoustic metamaterials with soft materials. For instance, soft materials have been used to create a significant contrast in impedance to achieve Mie resonances [27]. Soft materials gain an edge over traditional hard materials such as silicon and copper [28,29] through compliance and stimuli-responsiveness. Compliance enables soft materials to generate large elastic deformation [30] and diverse instability patterns [31]. The stimuli-responsiveness makes active control possible over the dynamic properties of the system, such as resonant frequency [32], damping [33], band structure and gap width of phononic crystals [34], etc., which brings many potential extensions to existing applications, such as metamaterials for waveguiding and localization [35], sensors [36], and wave rectification [37,38]. Despite the advantages, a problem that has hindered soft materials from being broadly applied in the dynamic and wave propagation applications is their high damping. A systematic study of the

dynamic properties, especially damping, of hydrogels and soft materials, is in increasing need.

Despite the importance, very few studies have been conducted within this area. To the authors' knowledge, there has not been an effort to quantify damping of hydrogels or to compare with other soft materials. Specifically, we are interested in the fundamental bending (flexural) vibration mode, and to this end, we use a simple setup with clamped–clamped boundary conditions under base excitation. Low-amplitude (linear) horizontal base excitations are carried out for vertically mounted samples in the frequency range covering the first bending mode of each sample. The first bending resonance neighborhood is recorded and fitted with the Euler–Bernoulli beam model to extract the modal viscous damping ratio, which is related to the structural damping. We carry out the measurements on the most commonly used hydrogel, the polyacrylamide (PAAm) gel with three different compositions and the widely used silicon-based organic elastomer, the Polydimethylsiloxane (PDMS), with two different compositions (Fig. 1b). By comparing the results on hydrogels and PDMS, we conclude that although gels are softer in terms of modulus, they have lower damping ratio, which is opposite to the modulus-damping relations of most conventional materials. This result shows that hydrogels are potential new materials for dynamic applications such as active wave guiding, localization, sensing, harvesting, and insulation.

2. Material and methods

2.1. Fabrication of PAAm hydrogel samples and PDMS samples

To characterize the damping ratio of gels, beam-shaped polyacrylamide (PAAm) gel samples are prepared. A 50% (w/w) glycerol solution (99% Sigma Aldrich, Catalog # G7757, Batch SHBK7272, CAS: 56-81-5) is prepared as the solvent instead of the pure water to prevent drying of the gels during testing in air. The monomer acrylamide (98% Sigma Aldrich, Catalog # O1700, Batch BCBZ5156, CAS:79-06-1) is dissolved in glycerol solution of the required weight according to different recipes. The crosslinker agent N,N'-Methylenebisacrylamide (Bis) (99% Sigma Aldrich, Catalog # 146072, Batch MKCC5908, CAS: 110-26-9) is dissolved in deionized water with a mass percentage of 2%. The two solutions are fully mixed to realize the mass concentration of acrylamide and Bis to be (i) 25%/1.2%, (ii) 25%/0.8%, and (iii) 25%/0.06%. The initiator ammonium persulfate (APS) (98% Sigma Aldrich, Catalog # A3678, Batch MKCG5404, CAS: 7727-54-0) is dissolved in deionized water with a concentration of 40 μg/mL. A 125 μL of the APS solution and 5 μL of catalyst tetramethylethylenediamine (TEMED) (99% Sigma Aldrich, Catalog # T7024, Batch MKCF5518, CAS: 110-18-9) are added to every 5.385 mL of the mixture. The mixture is injected with N_2 gas for 30 min and poured into a glass mold with a thickness of 2 mm. To guarantee complete curing, the mixture is left without disturbance for 1 h at room temperature, which is around 22 ° C. The cured hydrogel is then taken out of the mold and cut into rectangular prisms. The cut samples are put into 50% (w/w) glycerol solution for 24 h to guarantee fully swollen. The dimension of each sample ($L \times b \times h$) is measured after it is fully saturated (Fig. 1a). The weight of the sample is also measured by a digital balance, and the density values are obtained by averaging three samples for each composition. The polymer weight concentration of the gels in the swollen states are also calculated. The results are shown in Table 1.

We also prepare the polydimethylsiloxane (PDMS) samples. The base polymer agent and the curing agent from PDMS Kit Sylgard 184 (Electron Microscopy Sciences, Catalog # 24236-10, Batch 181002) are mixed with a mass ratio of (i) 10:1 and (ii) 20:1 compositions. The mixture is degassed in a vacuum chamber

for 1 h and poured into the glass mold with spacing 2 mm. The mold is put into the oven for curing at 60 ° C for 1 h. The PDMS samples after curing are cut into rectangular prisms. The dimensions ($L \times b \times h$) of the samples are measured (Fig. 1b). The weight is measured by a digital balance to obtain the density. The mass densities of each composition are averaged over three samples. The density values, polymer concentrations and sample dimensions are shown in Table 1.

2.2. Tensile test

To get reference values of Young's modulus of the samples, we conduct a series of uniaxial tensile tests on the Instron Model 5944 Universal Test System. A 2kN load cell is used for testing PDMS samples and a 5N load cell is used for hydrogel samples. Loading speed is set to be 0.2 mm/s and the total strain is restrained to be below 10% to ensure a linear response. During loading, both force $F(N)$ and displacement $u(mm)$ are recorded. The Young's modulus E is obtained through $E = FL/uA$, where $A = b \times h$ is the cross-sectional area and L is the length of the sample.

2.3. Dynamic testing

2.3.1. Dynamic testing setup

Various methods exist for viscous damping identification, such as the logarithmic decrement using free vibration data or half-power points method using steady-state harmonic frequency response data [39]. In the experiments here, frequency response function (FRF) plots are obtained around the first bending mode, and model simulations are matched with the experimental data to identify elastic modulus and viscous damping ratio (knowing the mass density and resonance frequency for each sample). A schematic of the experimental setup for the dynamic testing of the soft materials (hydrogel and PDMS samples) for bending vibrations is shown in Fig. 2. The sample is clamped at both ends to create fixed–fixed boundary conditions. Unlike cantilevered stiff materials [40] tested in vertical direction for damping identification (i.e. excitation parallel to the gravitational field), soft materials do not have sufficient bending stiffness to sustain its weight. Hence we clamp both ends of the soft material samples vertically for horizontal base excitation to minimize the gravity effect. The clamped sample is mounted on the armature of the APS-113 long-stroke shaker to provide base excitation in the form of white noise over the frequencies of interest. An accelerometer is attached to the base clamp to measure the base excitation. The velocity of the sample at a single point is measured using a laser Doppler vibrometer (LDV). The velocity and base acceleration are acquired through the data acquisition card (NI DAQ 4431) and the FRF is calculated in LabVIEW Signal Express. The experimental setup is shown in Fig. 3 along with a close-up view of a hydrogel sample in the clamps (not to scale) for horizontal base excitation.

2.3.2. Extraction of material parameters

The clamped–clamped configuration shown in Figs. 2 and 3 is modeled here as a uniform beam based on the Euler–Bernoulli beam theory (which is justified given the lower vibration mode and relatively high length to thickness ratio). This is a reasonable assumption since the experimental samples are thin beams, deformations are small, and the material is assumed to exhibit geometrically linear behavior. For a clamped–clamped Euler–Bernoulli beam, the transverse displacement (relative to the moving base) per translational base acceleration FRF, , can be obtained as

$$\beta(x, \omega) = \sum_{r=1}^{\infty} \frac{\sigma_r \phi_r(x)}{\omega_r^2 - \omega^2 + i2\zeta_r \omega_r \omega} \tag{1}$$

Table 1
Sample dimensions, density, and Young's modulus.

	Hydrogel 1.2% Bis	Hydrogel 0.8% Bis	Hydrogel 0.06% Bis	PDMS 10:1	PDMS 20:1
Length (mm)	49.8 ± 0.3	50 ± 0.1	49.7 ± 0.4	49.1 ± 0.4	49.6 ± 0.2
Width (mm)	3.9 ± 0.5	4.3 ± 0.4	4.0 ± 0.5	3.3 ± 0.2	2.7 ± 0.1
Thickness (mm)	2.5 ± 0.1	2.7 ± 0.1	3.4 ± 0.2	2.3 ± 0.1	2.3 ± 0.1
Mass density (kg m^{-3})	1190 ± 109	1185 ± 132	1179 ± 117	1057 ± 37	1119 ± 46
Polymer weight % after swelling	10.8	7.5	3.3	/	/
Young's modulus E from tensile testing (kPa)	293 ± 23	193 ± 6	15 ± 1	1956 ± 126	946 ± 89
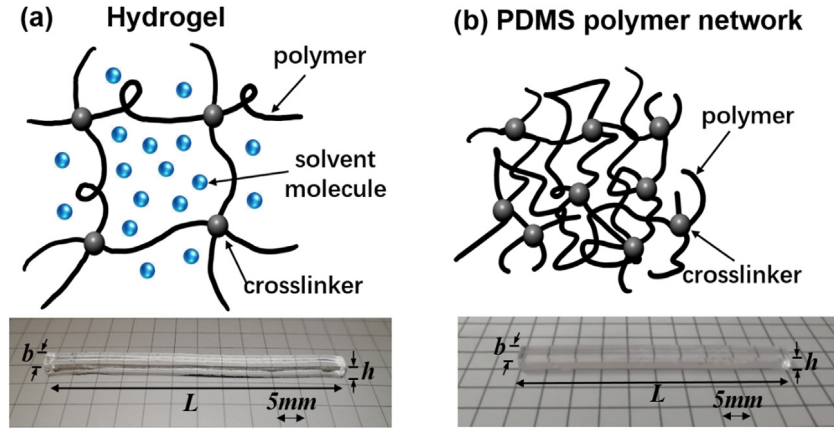
Fig. 1. Schematic of the molecular structures and the photo of the (a) hydrogel and (b) PDMS samples.
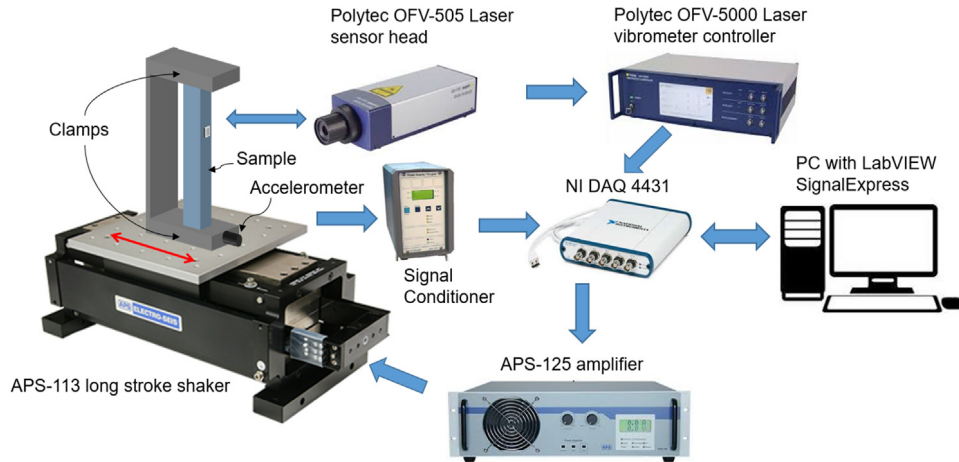
Fig. 2. Experimental schematic for dynamic base excitation of hydrogel and PDMS samples around for the first bending mode (sample not to scale).
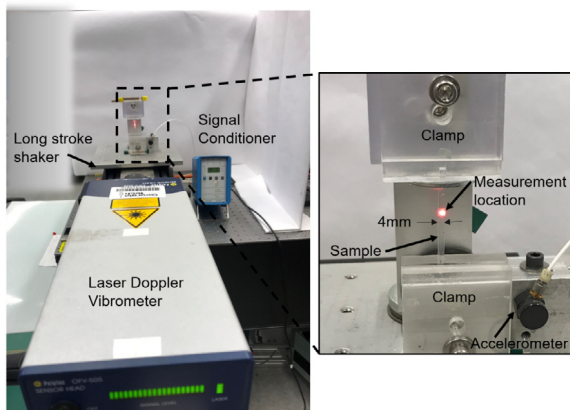
Fig. 3. Experimental setup with a close-up view of a sample (hydrogel) and clamps.

where

$$\sigma_r = -m \int_0^L \phi_r(x)dx \tag{2}$$

and the mass normalized eigenfunction mode shape for the rth mode is

$$\phi_r(x) = \frac{1}{\sqrt{mL}} \left[\cos \frac{\lambda_r x}{L} - \cosh \frac{\lambda_r x}{L} \right.$$
$$\left. - \frac{\sin \lambda_r + \sinh \lambda_r}{\cos \lambda_r - \cosh \lambda_r} \left(\sin \frac{\lambda_r x}{L} - \sinh \frac{\lambda_r x}{L} \right) \right] \tag{3}$$

where $m = \rho bh$ is the mass per unit length of the beam and the eigenvalues ($\lambda_r > 0, r = 1, 2, \ldots$) are the roots of the characteristic equation (for clamped–clamped boundary conditions):

$$1 - \cos \lambda_r \cosh \lambda_r = 0 \tag{4}$$

The natural frequencies of the beam are then

$$\omega_r = \lambda_r^2 \sqrt{\frac{EI}{mL^4}} \tag{5}$$

where E is the modulus of elasticity (i.e. Young's modulus) and $I = bh^3/12$ is the second moment of area for a rectangular cross-section. In the experiments, the focus is placed on the first vibration mode, i.e. $r = 1$.

Note that the velocity measurement taken by the LDV in the experiments is the absolute velocity response of the beam in the inertial reference frame (rather than relative to the moving base). Therefore, the relative displacement FRF given by Eq. (1) must be modified to express the absolute velocity response of the beam:

$$\beta_{absVel} = \frac{1}{j\omega} + j\omega\beta(x, \omega) \tag{6}$$

where $x = L_m$ is the point of the velocity measurement in the experiments.

The Euler–Bernoulli model given by Eqs. (1)–(6) is used to extract the elastic modulus and damping ratio from the experimental data. Using the experimental FRF along with the measured dimensions and mass density in Eq. (5), the elastic modulus can be determined. The modal damping ratio is determined by fitting the Euler–Bernoulli model to the experimental data using Eqs. (1) and (6). While viscous damping is a standard model, another damping model would be to assume structural damping, in which case the FRF given by Eq. (1) becomes:

$$\beta^*(x, \omega) = \sum_{r=1}^{\infty} \frac{\sigma_r \phi_r(x)}{(1 + i\gamma)\omega_r^2 - \omega^2} \tag{7}$$

where γ is the structural damping factor related to the complex part of the modulus of elasticity ($\gamma = \tan\delta$ in terms of the loss tangent). Note that the viscous damping and structural damping models [40] can be bridged to one another at $\omega = \omega_r$ with $2\zeta_r = \gamma$ in view of Eqs. (1) and (7), where the focus is placed on the first bending mode ($r = 1$) in this work.

3. Results and discussion

The hydrogel samples of 25% PAAm/1.2% Bis, 25% PAAm/ 0.8% Bis, 25% PAAm/ 0.06% Bis and the PDMS samples of 10:1 and 20:1 base to curing agent ratio are tested. Three samples of each hydrogel composition and PDMS composition are tested. The three samples are cut from the same batch of gel or PDMS. One dynamic test is performed on each sample, and the error bar comes from sample to sample variation. Fig. 4 shows one representative curve of the dynamic testing results of each hydrogel and PDMS composition and the Euler–Bernoulli fitting results for each case. Based on the Euler–Bernoulli model, the damping ratio ζ (from the first bending mode) and Young's modulus are extracted for each sample and averaged for each composition. The extracted values are shown in Table 2.

The Young's modulus extracted from dynamic testing can be compared with those from tensile testing (Table 1) for validation. From both tests, the extracted Young's modulus increases as the crosslinker density increases for both hydrogels and PDMS samples. The values extracted from the two independent methods agree reasonably well. There are some discrepancies. It could be due to the sample to sample variation. The multiple samples prepared for dynamic testing are cut from the same big piece of gel, while the samples prepared for tensile testing are cut from a different piece of gel. Both PDMS and PAAm gels are synthesized through radical polymerization which naturally would introduce sample-to-sample variation. The error may also be introduced during the chemical weighting process, as the weight of some of the constituents, for instance, Bis, is below 1 mg which is hard to be weighed accurately. Another origin of the discrepancy may be from the idealized clamped–clamped boundary conditions in the analysis of the dynamic testing results. Because the samples are soft, they can easily generate creases and local large deformation near the clamped region. Despite our efforts in keeping the condition as close to the clamped–clamped condition as possible, in reality, it may still deviate from the perfect clamped–clamped condition. Mathematically speaking, any deviation from this ideal boundary condition (assumed in the Euler–Bernoulli model) would change the characteristic equation of the eigenvalues (Eq. (4)), which would in turn affect the identified elastic modulus. Nonetheless, we get reasonable agreement between the modulus values obtained from the two independent testing techniques, with the largest discrepancy that appears for the softest gel samples is 44%. The discrepancies for other samples are much smaller.

The main purpose of this study is to characterize the structural damping of hydrogels and explore how it differs from elastomers such as PDMS. The dynamic testing results give a very consistent measure of the damping values, with very small error bars between measurements and a clear difference between hydrogel and PDMS as can be seen in Table 2. For better visualization, in Fig. 5, we show a comparison of the FRFs for the hydrogel and PDMS samples. The data of the five samples corresponding to three hydrogel compositions and two PDMS compositions are plotted. The frequency for each composition is normalized by its resonant frequency to better illustrate the magnitude of the quality factor. The narrower the peak width and the greater the peak value, the greater the quality factor and equivalently, the less the damping ratio. It can be observed clearly from the peak sharpness that the damping of hydrogels is significantly less than that of PDMS. Besides, based on the peak heights of the hydrogels of different compositions, a conclusion can be drawn that the samples with higher crosslink density, which results in higher stiffness, have lower damping ratio.

There are two possible dissipation mechanisms in hydrogels. Gels are composed of crosslinked polymer networks and solvent molecules (Fig. 1a). One source of dissipation could be the friction between the polymer chains when the polymers reconfigure, and the other is the friction between the polymers and the solvent when the solvent migrates through the polymer network. The two mechanisms give rise to macroscopic viscoelastic and poroelastic behaviors respectively [41,42]. From our previous study [43–45], it has been shown that the viscoelastic effect of a swollen PAAm gel is negligible. The reason is that more than 95% of the gel content is water and the network is highly straightened due to swelling, so chances are low for the polymer chains to rub against each other during deformation. Comparatively, the poroelastic behavior related to solvent transport in the network is more dominant in gels. In our previous work, we have measured that the typical diffusivity of solvent in PAAm gel is in the order of $D = 10^{-10}$ m^2/s. The thickness of the PAAm gel sample tested in this study is around $h = 3 \times 10^{-3}$ m. Therefore, the poroelastic response time scale is around $t = h^2/D = 9 \times 10^4$ s. The structural vibration carried out in this study is in the frequency range of tens of Hz, which is far away from the poroelastic time scale. Therefore, in this frequency range, the gel behaves mostly like an elastic material without much dissipation. On the contrary, the polymer chains are more densely packed in elastomers such as PDMS (Fig. 1b), and the viscoelastic behavior of the material is more significant. Conclusively, the intrinsic difference in the molecular structures between gels and elastomers determines the difference in their damping behaviors — significantly lower damping in hydrogels than in PDMS. The damping of polymers and polymeric gels can be related to many factors: the polymer
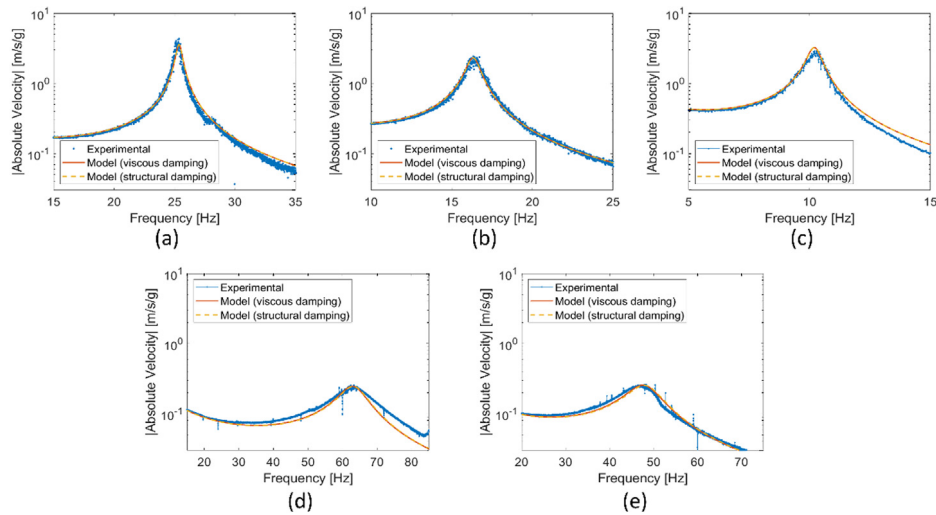
Fig. 4. Velocity FRFs (experimental vs. model) for (a) hydrogel 1.2% Bis, (b) hydrogel 0.8% Bis, (c) hydrogel 0.06% Bis, (d) PDMS 10:1, and (e) PDMS 20:1.

Table 2
Extracted damping ratio and Young's modulus values of hydrogels and PDMS samples from the dynamic testing.

	Hydrogel 1.2% Bis	Hydrogel 0.8% Bis	Hydrogel 0.06% Bis	PDMS 10:1	PDMS 20:1
Damping ratio, ζ	0.0156 ± 0.0049	0.0194 ± 0.0059	0.0276 ± 0.0012	0.0759 ± 0.0085	0.0796 ± 0.0014
Young's modulus Y (kPa)	219 ± 41	122 ± 32	27 ± 6	2271 ± 117	1509 ± 64

concentration, polymer chain length, network topologies and the interaction properties between the polymers and solvent. The subject itself is complex enough to deserve many future works to follow. Based on the current results, it seems to indicate that among the different compositions of hydrogels and PDMS, the one with lower crosslink density has higher damping (Table 2). It might be because as the crosslink density decreases, the polymer chains between two crosslinkers are longer and more coiled chains may be developed. Also, as the crosslinker to monomer ratio increases, the crosslinking efficiency during curing may become lower, causing more dangling chains and side chains to be developed. These factors may attribute to higher viscoelastic characteristics of the network. Additionally it is known that the water molecules near the polymers in the hydrogels are less mobile because of the hydrogen interactions between water molecules and the polymers [46]. Therefore, for hydrogels with lower crosslink densities, the water concentration is higher (Table 1), and there exists more mobile water molecules that could cause more viscous dissipation. It might be another reason for the higher damping in the hydrogels of lower crosslink densities. Summarily, the current results clearly show that the presence of solvent in the polymer network can significantly reduce the damping of the polymeric materials, but the detailed relation between molecular structures and the macroscopic damping of hydrogels requires more systematic studies in the future.

The key observation of this study that hydrogels have much lower damping than PDMS despite the modulus of hydrogels being much lower than PDMS is, in fact, contradictory to most materials' behaviors. An Ashby plot of the mechanical loss coefficient $\tan \delta = 2\zeta$ against Young's modulus for many different materials, ranging from ceramics, metals, and alloys to soft materials such as elastomers, biological materials, PDMS and hydrogels is drawn in Fig. 6. The data was collected from Cambridge Engineering Selector (CES) EduPack software [47]. A tendency line $E \tan \delta = 0.02$ is introduced, beneath which materials tend to be softer and less damped, and above it, the materials tend to be stiffer and more damped. In general, stiffer materials tend to be less damped and softer materials tend to be more damped. Most of the materials fall on the tendency line, such as ceramics, metals and
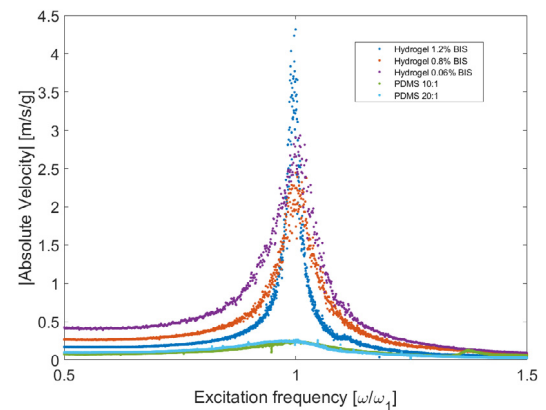
Fig. 5. Velocity FRF comparison of hydrogel and PDMS samples.

hard composites. However, hydrogel stands out as unusually soft materials with relatively low damping. Compared to other soft materials such as PDMS, rubbers, and other polymeric materials, the hydrogel is less dissipative and softer at the same time. Plus, hydrogels are biocompatible and stimuli-responsive. All these characteristics indicate that hydrogels are potentially useful in future applications related to dynamic problems involving passive and active wave guiding and manipulation.

4. Conclusion

This work characterizes the dynamic properties of extremely soft materials. The hydrogel and PDMS samples of different compositions are clamped vertically and excited horizontally during the dynamic testing. Young's modulus and structural damping are extracted from the dynamic test. The Young's modulus value of each sample is compared with a separate uniaxial tensile test for verification. The result proves the reliability of the dynamic method. In experiments, hydrogels samples of three compositions
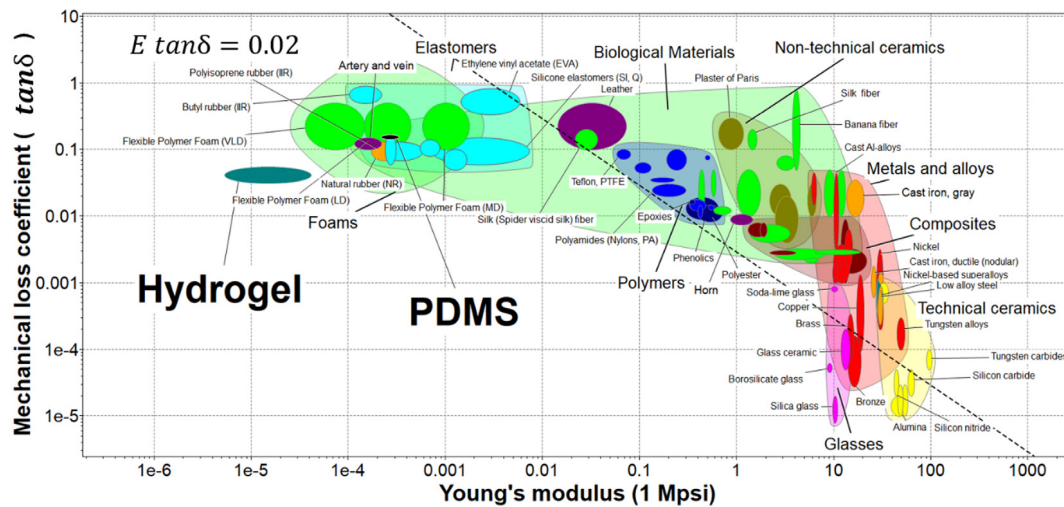
Fig. 6. Ashby plot of mechanical loss coefficient over Young's modulus.

and PDMS samples of two compositions are tested. In comparison, PAAm gels are significantly less damped than PDMS even though PAAm gels are much softer than PDMS. Gels are compliant, bio-compatible and stimuli-responsive and also stand out from other soft elastomeric materials due to its low damping. As a result, hydrogels can sustain wave and vibrational energy flow better than most other soft and lossy materials. Additionally, hydrogels can be easily 3D printed. All these characteristics of gels provide new opportunities in designing future stimuli-responsive metamaterials and phononic crystals for wave guiding, focusing, and localization, among other applications.

Declaration of competing interest

The authors declare that they have no known competing financial interests or personal relationships that could have appeared to influence the work reported in this paper.

Acknowledgments

References

[1] E. Tian, J. Wang, Y. Zheng, et al., Colorful humidity sensitive photonic crystal hydrogel, J. Mater. Chem. 18 (10) (2008) 1116–1122.

[2] N. Sarkar, Thermal gelation properties of methyl and hydroxypropyl methylcellulose, J. Appl. Polym. Sci. 24 (4) (1979) 1073–1087.

[3] L. Brannon-Peppas, N.A. Peppas, Equilibrium swelling behavior of pH-sensitive hydrogels, Chem. Eng. Sci. 46 (3) (1991) 715–722.

[4] M. Dehghany, H. Zhang, R. Naghdabadi, et al., A thermodynamically-consistent large deformation theory coupling photochemical reaction and electrochemistry for light-responsive gels, J. Mech. Phys. Solids 116 (2018) 239–266.

[5] G. Albin, T.A. Horbett, B.D. Ratner, Glucose sensitive membranes for controlled delivery of insulin: insulin transport studies, J. Control. Release 2 (1985) 153–164.

[6] K. Ishihara, M. Kobayashi, N. Ishimaru, et al., Glucose induced permeation control of insulin through a complex membrane consisting of immobilized glucose oxidase and a poly (amine), Polym. J. 16 (8) (1984) 625.

[7] T. Tanaka, I. Nishio, S.T. Sun, et al., Collapse of gels in an electric field, Science 218 (4571) (1982) 467–469.

[8] D.J. Beebe, J.S. Moore, J.M. Bauer, et al., Functional hydrogel structures for autonomous flow control inside microfluidic channels, Nature 404 (6778) (2000) 588.

[9] Y. Qiu, K. Park, Environment-sensitive hydrogels for drug delivery, Adv. Drug Deliv. Rev. 53 (3) (2001) 321–339.

[10] J. Li, D.J. Mooney, Designing hydrogels for controlled drug delivery, Nat. Rev. Mater. 1 (12) (2016) 16071.

[11] A. Loebsack, K. Greene, S. Wyatt, et al., In vivo characterization of a porous hydrogel material for use as a tissue bulking agent, J. Biomed. Mater. Res. 57 (4) (2001) 575–581.

[12] J. Shin, P.V. Braun, W. Lee, Fast response photonic crystal ph sensor based on templated photo-polymerized hydrogel inverse opal, Sensors Actuators B 150 (1) (2010) 183–190.

[13] Y. Tai, M. Mulle, I.A. Ventura, et al., A highly sensitive, low-cost, wearable pressure sensor based on conductive hydrogel spheres, Nanoscale 7 (35) (2015) 14766–14773.

[14] D. Buenger, F. Topuz, J. Groll, Hydrogels in sensing applications, Prog. Polym. Sci. 37 (12) (2012) 1678–1719.

[15] S. Maeda, Y. Hara, T. Sakai, et al., Self-walking gel, Adv. Mater. 19 (21) (2007) 3480–3484.

[16] H. Yuk, S. Lin, C. Ma, et al., Hydraulic hydrogel actuators and robots optically and sonically camouflaged in water, Nat. Commun. 8 (2017) 14230.

[17] Z. Lei, Q. Wang, S. Sun, et al., A bioinspired mineral hydrogel as a self-healable, mechanically adaptable ionic skin for highly sensitive pressure sensing, Adv. Mater. 29 (22) (2017) 1700321.

[18] M. Liao, P. Wan, J. Wen, et al., Wearable, healable, and adhesive epidermal sensors assembled from mussel-inspired conductive hybrid hydrogel framework, Adv. Funct. Mater. 27 (48) (2017) 1703852.

[19] A.E. Forte, S. Galvan, F. Manieri, et al., A composite hydrogel for brain tissue phantoms, Mater. Des. 112 (2016) 227–238.

[20] M. Liu, Y. Ishida, Y. Ebina, et al., An anisotropic hydrogel with electrostatic repulsion between cofacially aligned nanosheets, Nature 517 (7532) (2015) 68.

[21] H. Saraf, K.T. Ramesh, A.M. Lennon, et al., Mechanical properties of soft human tissues under dynamic loading, J. Biomech. 40 (9) (2007) 1960–1967.

[22] F. Pervin, W.W. Chen, Dynamic mechanical response of bovine gray matter and white matter brain tissues under compression, J. Biomech. 42 (6) (2009) 731–735.

[23] T.C. Ning, D.M. Atkins, R.C. Murphy, Bladder explosions during transurethral surgery, J. Urol. 114 (4) (1975) 536–539.

[24] T. Klekiel, R. Będziński, Finite element analysis of large deformation of articular cartilage in upper ankle joint of occupant in military vehicles during explosion, Arch. Metall. Mater. 60 (3) (2015) 2115–2121.

[25] J. Ophir, I. Cespedes, H. Ponnekanti, et al., Elastography: a quantitative method for imaging the elasticity of biological tissues, Ultrason. Imaging 13 (2) (1991) 111–134.

[26] J. Ophir, S.K. Alam, B. Garra, et al., Elastography: ultrasonic estimation and imaging of the elastic properties of tissues, Proc. Inst. Mech. Eng. H 213 (3) (1999) 203–233.

[27] T. Brunet, A. Merlin, B. Mascaro, et al., Soft 3D acoustic metamaterial with negative index, Nat. Mater. 14 (4) (2015) 384.

[28] R.A. Shelby, D.R. Smith, S. Schultz, Experimental verification of a negative index of refraction, Science 292 (5514) (2001) 77–79.

[29] Y. Liu, X. Zhang, Metamaterials: a new frontier of science and technology, Chem. Soc. Rev. 40 (5) (2011) 2494–2507.

[30] A. Evgrafov, C.J. Rupp, M.L. Dunn, et al., Optimal synthesis of tunable elastic wave-guides, Comput. Methods Appl. Mech. Engrg. 198 (2) (2008) 292–301.

[31] K. Bertoldi, M.C. Boyce, Mechanically triggered transformations of phononic band gaps in periodic elastomeric structures, Phys. Rev. B 77 (5) (2008) 052105.

[32] J. Zhu, S. Cai, Z. Suo, Resonant behavior of a membrane of a dielectric elastomer, Int. J. Solids Struct. 47 (24) (2010) 3254–3262.

[33] S.M. Clarke, A.R. Tajbakhsh, E.M. Terentjev, et al., Soft elasticity and mechanical damping in liquid crystalline elastomers, J. Appl. Phys. 89 (11) (2001) 6530–6535.

[34] Q. Zhang, K. Zhang, G. Hu, Tunable fluid-solid metamaterials for manipulation of elastic wave propagation in broad frequency range, Appl. Phys. Lett. 112 (22) (2018) 221906.

[35] S. Zhang, L. Yin, N. Fang, Focusing ultrasound with an acoustic metamaterial network, Phys. Rev. Lett. 102 (19) (2009) 194301.

[36] R. Lucklum, J. Li, Phononic crystals for liquid sensor applications, Meas. Sci. Technol. 20 (12) (2009) 124014.

[37] L. Zigoneanu, B.I. Popa, S.A. Cummer, Three-dimensional broadband omnidirectional acoustic ground cloak, Nat. Mater. 13 (4) (2014) 352.

[38] B. Liang, B. Yuan, J. Cheng, Acoustic diode: rectification of acoustic energy flux in one-dimensional systems, Phys. Rev. Lett. 103 (10) (2009) 104301.

[39] Leonard Meirovitch, Fundamentals of Vibrations, Waveland Press, 2010.

[40] V.N. Paimushin, et al., Theoretical-experimental method for determining the parameters of damping based on the study of damped flexural vibrations of test specimens. 1. Experımental basıs, Mech. Compos. Mater. 50 (2) (2014) 127–136.

[41] Y. Hu, Z. Suo, Viscoelasticity and poroelasticity in elastomeric gels, Acta Mech. Solida Sin. 25 (2012) 441–457.

[42] D. He, Y. Hu, Nonlinear visco-poroelasticity of gels with different rheological parts (submitted for publication).

[43] Y. Lai, Y. Hu, Probing the swelling-dependent mechanical and transport properties of polyacrylamide hydrogels through AFM-based dynamic nanoindentation, Soft Matter 14 (2018) 2619–2627.

[44] Y. Lai, Y. Hu, Unified solution of poroelastic oscillation indentation on gels for spherical, conical and cylindrical indenters, Soft Matter 13 (2017) 852–861.

[45] Y. Hu, X. Zhao, J.J. Vlassak, Z. Suo, Using indentation to characterize the poroelasticity of gels, Appl. Phys. Lett. 96 (2010) 121904.

[46] P.A. Netz, T. Dorfmüller, J. Phys. Chem. B 102 (1998) 4875.

[47] M.F. Ashby, H.R. Shercliff, Cambridge Engineering Selector (CES) Edupack, 2005.